CL-150557 Received: June 6, 2015 | Accepted: June 26, 2015 | Web Released: October 5, 2015

Synthesis and Acid-responsive Electron-transfer Disproportionation of Non- and Tetramesityl-substituted 1,1′,9,9′-Bicarbazole

Palash Pandit,[1] Toshikazu Nakamura,[1] and Shuhei Higashibayashi*[1,2]
[1]*Institute for Molecular Science, 5-1 Higashiyama, Myodaiji, Okazaki, Aichi 444-8787*
[2]*Japan Science and Technology Agency, ACT-C, 4-1-8 Honcho, Kawaguchi, Saitama 332-0012*

(E-mail: higashi@ims.ac.jp)

Non-substituted 1,1′,9,9′-bicarbazole and 3,3′,6,6′-tetramesityl-1,1′,9,9′-bicarbazole were synthesized through dimerization of carbazole derivatives and oxidative N–N bond formation reaction. Non-substituted 1,1′,9,9′-bicarbazole formed a stacking packing structure in crystal. Both bicarbazoles were found to undergo acid-responsive electron-transfer disproportionation. The radical cation generated from the non-substituted 1,1′,9,9′-bicarbazole was stable in solution under air at room temperature, even without protecting bulky substituents.

Recently, we have reported the acid-responsive electron-transfer disproportionation of a bicarbazole derivative **1a** and a biacridine derivative **2a** with *t*-butyl substituents through the acid-regulated ring-opening/closing reactions (Figure 1 and Scheme 1).[1] Since the acid-responsive property is a novel finding, the scope and limitation of the compounds have not yet been revealed fully. During the course of our study on **1a** with *t*-butyl substituents, we also investigated non-substituted bicarbazole **1b** and 3,3′,6,6′-tetramesityl-substituted bicarbazole **1c**, and found that they also undergo the acid-responsive electron-transfer disproportionation. Here, we report the syntheses of **1b** and **1c**, the crystal structure of **1b**, their acid-responsiveness, and the stability of the radical cation of **1b**.

1b and **1c** were synthesized as shown in Scheme 2. 3,3′,6,6′-Tetra-*t*-butyl-1,1′-bicarbazole (**3a**) was prepared according to the reported procedure.[1] *t*-Butyl groups of **3a** were removed by refluxing with $AlCl_3$ in benzene, to afford the non-substituted **3b** in 65% yield. Oxidative coupling of **3b** afforded non-substituted **1b** in 24% yield. 3,3′,6,6′-Tetramesityl-1,1′,9,9′-bicarbazole **1c** was synthesized from dibromocarbazole **4**[2] (Scheme 2). Suzuki–Miyaura cross-coupling between **4** and 2,4,6-trimethylphenylboronic acid afforded dimesitylcarbazole **5**, which was further converted to bromodimesitylcarbazole **6** by monobromination. Dimer **7** was obtained in 40% yield by oxidative coupling of **6** at nitrogen atom using $KMnO_4$[3] in acetone. Ni(0)-mediated reductive cyclization of **7** did not afford the desired **1c** but only **3c** in 20% yield, with recovered **7**, due to the reductive cleavage of the N–N bond. The N–N bond of **7** seems to be weaker to the reductive condition than that of the corresponding derivative with stronger electron-donating *t*-butyl substituents.[1] Thus, the C–C bond was first connected by Ni(0)-

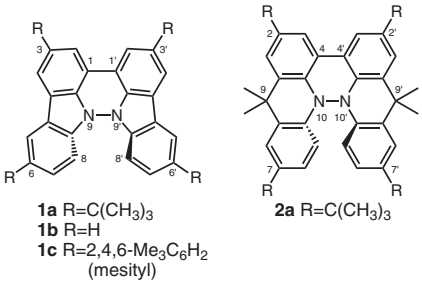

Figure 1. 1,1′,9,9′-Bicarbazole derivatives **1** and 4,4′,10,10′-biacridine derivatives **2**.

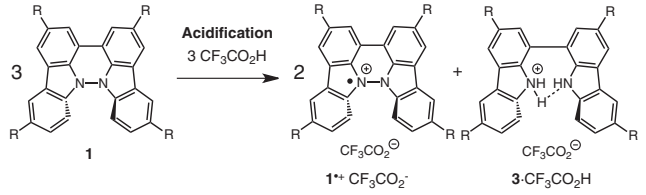

Scheme 1. Acid-responsive electron-transfer disproportionation of bicarbazole **1**.

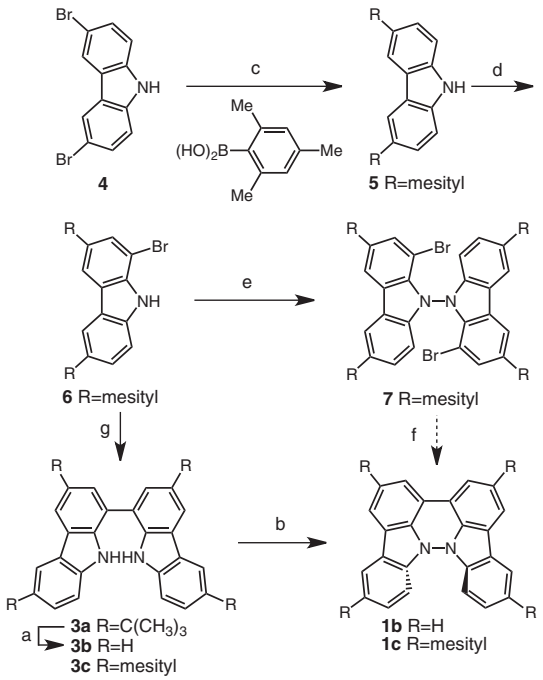

Scheme 2. Reagents and conditions: (a) $AlCl_3$ 600 mol %, benzene, 80 °C, 3 h, 65%; (b) **3b**, Bu_4NMnO_4 220 mol %, pyridine, 70 °C, 24 h, 24%, **3c**, Bu_4NMnO_4 200 mol %, pyridine, 70 °C, 24 h, 49%; (c) 2,4,6-$Me_3C_6H_2B(OH)_2$ 300 mol %, $[Pd(PPh_3)_4]$ 2 mol %, Cs_2CO_3 300 mol %, toluene:EtOH:H_2O = 3:1:1, 100 °C, 24 h, 68%; (d) *N*-bromosuccinimide 110 mol %, SiO_2, CH_2Cl_2, rt, 6 h, 90%; (e) $KMnO_4$ 250 mol %, acetone, 60 °C, 6 h, 40%; (f) Ni(1,5-cyclooctadiene)$_2$ 150 mol %, 1,5-cyclooctadiene 150 mol %, 2,2′-bipyridyl 150 mol %, THF, 55 °C, 24 h; (g) Ni(1,5-cyclooctadiene)$_2$ 300 mol %, 1,5-cyclooctadiene 300 mol %, 2,2′-bipyridyl 300 mol %, THF, 80 °C, 3 h, 89%.

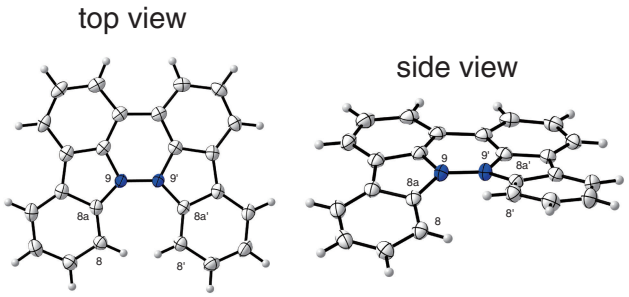

Figure 2. ORTEP drawings of **1b** at 50% probability level obtained by X-ray crystallographic analysis.

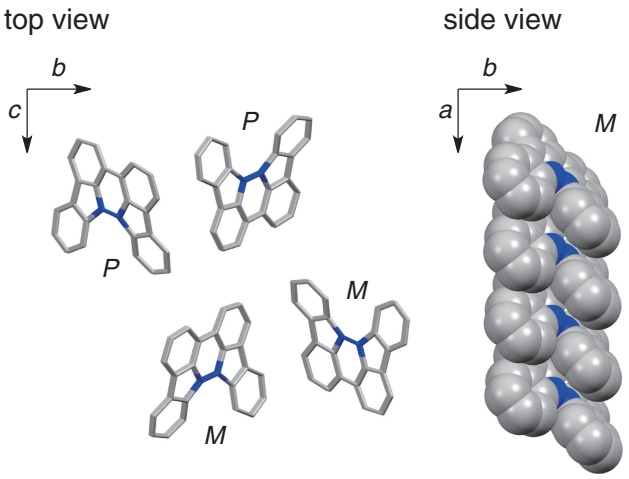

Figure 3. Top view of packing and side view of stacked column of **1b**.

Table 1. Structural parameters of **1a** and **1b**

	1a[a]	**1b**[a]	Calculated **1b**[b]
Distance of N_9–$N_{9'}$/Å	1.41	1.40	1.39
Dihedral angle of $\angle C_{8a}N_9N_{9'}C_{8a'}$/°	48	32	42
Distance of C_8–$C_{8'}$/Å	3.33	3.25	3.26

[a]X-ray structures. [b]ωB97Xd/6-31G(d).

mediated reductive coupling of **6**, giving the desired **3c** in 89% yield. Oxidative N–N bond formation of **3c** by $KMnO_4$ in acetone gave the desired **1c** in 7% yield. The conditions using Bu_4NMnO_4 in pyridine improved the yield up to 49%.

A single crystal of **1b** for X-ray crystallographic analysis was obtained (Figures 2, 3, and Supporting Information). The structural parameters of the X-ray structures of **1a**[1] and **1b**, and those of the calculated **1b** (ωB97Xd/6-31G(d)) are shown in Table 1. The dihedral angle $\angle C_{8a}N_9N_{9'}C_{8a'}$ of **1b** is significantly smaller than those of **1a** and the calculated **1b**. This difference is attributed to the effect of stacking of **1b** in crystal. While **1a** is not stacked in crystal due to the steric repulsion of the *t*-butyl groups,[1] **1b** is stacked with the same enantiomers in crystal, giving slipped columns (Figure 3). DFT calculation (ωB97Xd/6-31G(d)) shows that the racemization energy barrier of **1b** is only 5.2 kcal mol^{-1}, indicating the flexibility of the helical structure.

Both **1b** and **1c** exhibited acid-responsive property similar to that of **1a**, which underwent electron-transfer disproportionation upon the addition of acid. UV–vis–NIR spectrum of the yellow-colored solution of **1b** in CH_2Cl_2 showed absorption at 450 nm (Figure 4a), and the emission maximum was 503 nm (Figure 4b). The absorption band at 450 nm was decreased by the addition of CF_3CO_2H (TFA) and a new absorption maximum at 621 nm of $\mathbf{1b}^{\bullet+}$ was observed (Figure 4a), concomitant with the disproportionation of **1b**. The formation of $\mathbf{1b}^{\bullet+}$ was confirmed by the observation of the ESR spectrum (Figure 5a). The quenching experiment of the mixture by hydrazine afforded **1b** in 64% NMR yield and **3b** in 35% NMR yield, which reflects the formation of $\mathbf{1b}^{\bullet+}$ and protonated **3b** through the disproportionation reaction under acidic conditions. Similar results were observed for **1c** by the addition of CF_3CO_2H (Figures 5b and 6). Meanwhile, some difference in the acid responsiveness among **1a**, **1b**, and **1c** was observed, as shown in the generation of the radical cations depending on the amount of CF_3CO_2H in the UV–vis–NIR spectra (Figures 4a and 6a).[1] The order of the acid responsiveness was **1a**, **1c**, and **1b**, which could be attributed to the difference in the basicity caused by the substituents.

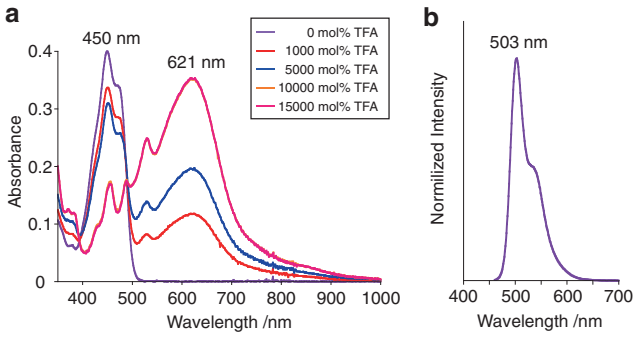

Figure 4. (a) UV–vis–NIR spectra of **1b** (0.05 mM) and **1b** with 1000, 5000, 10000, and 15000 mol% CF_3CO_2H in CH_2Cl_2. (b) Emission spectrum of **1b** (0.02 mM) in CH_2Cl_2 (excited at 450 nm).

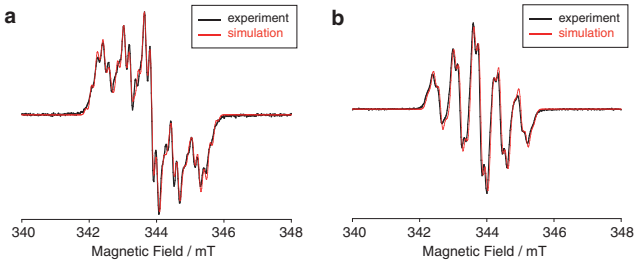

Figure 5. (a) ESR spectrum of **1b** (1.0 mM) with 2000 mol% CF_3CO_2H in CH_2Cl_2 at room temperature (X-band, $\nu = 9.639864$ GHz, $g = 2.00290$) and the simulated spectrum ($S = 1/2$, hyperfine coupling constants $a = 6.1$ G with 2 nitrogens and 2.2, 1.8, 1.6, 1.1, 0.3, 0.2, 0.1 G with 14 hydrogens) by *EasySpin*.[4] (b) ESR spectrum of **1c** (1.0 mM) with 2000 mol% CF_3CO_2H in CH_2Cl_2 at room temperature (X-band, $\nu = 9.637984$ GHz, $g = 2.00302$) and the simulated spectrum ($S = 1/2$, hyperfine coupling constants $a = 6.0$ G with 2 nitrogens and 1.8, 1.4, 0.2, 0.2, 0.2 G with 10 hydrogens) by *EasySpin*.[4]

In general, carbazole radicals are not stable enough to stay in solution under ambient atmosphere at room temperature, particularly without protecting substituents at the 1,3,6,8-

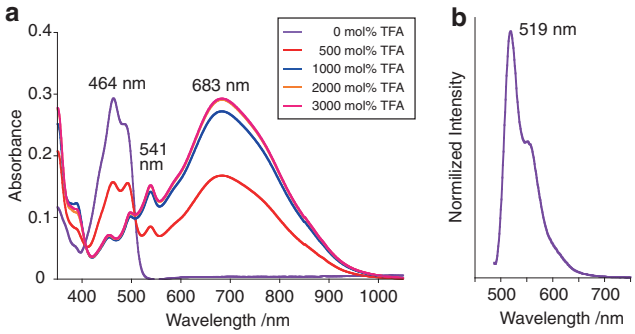

Figure 6. UV–vis–NIR spectra of **1c** (0.03 mM) with 0, 500, 1000, 2000, and 3000 mol % CF_3CO_2H in CH_2Cl_2. (b) Emission spectrum of **1c** (0.02 mM) in CH_2Cl_2 (excited at 464 nm).

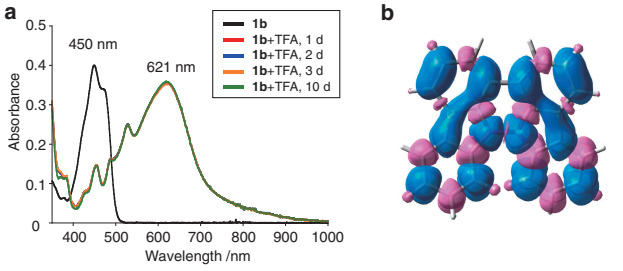

Figure 7. (a) UV–vis–NIR spectra of **1b** (0.05 mM) with 10000 mol % CF_3CO_2H in CH_2Cl_2 after 1, 2, 3, and 10 d at 20 °C under air. (b) Calculated spin density distribution of $BC^{\bullet+}$ [UωB97XD/6-31G(d)]. Blue and pink colors indicate the positive and negative spin density, respectively.

positions.[3,5] On the other hand, $\mathbf{1b}^{\bullet+}$ without substituents at the 3,3′,6,6′-positions showed high stability comparable to $\mathbf{1a}^{\bullet+}$.[1] UV–vis–NIR spectrum of $\mathbf{1b}^{\bullet+}$ generated from **1b** and CF_3CO_2H scarcely changed even after 10 days at room temperature under air (Figure 7a). The stability of $\mathbf{1b}^{\bullet+}$ under these conditions is comparable to that reported for $\mathbf{1a}^{\bullet+}$. The calculated spin density is delocalized over the bicarbazole skeleton (Figure 7b), which contributes to the thermodynamic stability of $\mathbf{1b}^{\bullet+}$ even without kinetic stabilization by substituents at the 3,3′,6,6′-positions. **1c** also showed comparable high stability (Supporting Information).

In summary, non-substituted (**1b**) and tetramesityl-substituted (**1c**) 1,1′,9,9′-bicarbazole were synthesized and found to undergo acid-responsive electron-transfer disproportionation, similar to tetra-*t*-butyl-substituted 1,1′,9,9′-bicarbazole **1a**. The generated radical cation of **1b** showed high stability comparable to **1a** without kinetic stabilization by substituents. **1b** without bulky substituents formed a π–π stacking columnar crystal structure, in contrast to the non-stacking crystal structure of **1a**. The pristine 1,1′,9,9′-bicarbazole **1b** would be useful as a synthetic intermediate for other substituted 1,1′,9,9′-bicarbazoles as well.

This work was supported by the Japan Society for the Promotion of Science (JSPS) KAKENHI Grant Numbers 25410124 (S. H.), 26102002 (S. H.), and 25287091 (T. N.). The computations were performed using Research Center for Computational Science, Okazaki, Japan. We thank S. Masaoka (IMS) for measurements of UV–vis–NIR spectra.

Supporting Information is available electronically on J-STAGE.

References

1 P. Pandit, K. Yamamoto, T. Nakamura, K. Nishimura, Y. Kurashige, T. Yanai, G. Nakamura, S. Masaoka, K. Furukawa, Y. Yakiyama, M. Kawano, S. Higashibayashi, *Chem. Sci.* **2015**, *6*, 4160.
2 L. Zhang, S. Zeng, L. Yin, C. Ji, K. Li, Y. Li, Y. Wang, *New J. Chem.* **2013**, *37*, 632.
3 F. A. Neugebauer, H. Fischer, S. Bamberger, H. O. Smith, *Chem. Ber.* **1972**, *105*, 2694.
4 S. Stoll, A. Schweiger, *J. Magn. Reson.* **2006**, *178*, 42.
5 J. F. Ambrose, L. L. Carpenter, R. F. Nelson, *J. Electrochem. Soc.* **1975**, *122*, 876.